Edge states and the integer quantum Hall conductance in spin-chiral ferromagnetic kagomé lattice

Zhigang Wang[1] and Ping Zhang[1,2,*]

[1]*LCP, Institute of Applied Physics and Computational Mathematics, P.O. Box 8009, Beijing 100088, People's Republic of China*

[2]*Center for Applied Physics and Technology, Peking University, Beijing 100871, People's Republic of China*

(Received 30 November 2007; revised manuscript received 11 January 2008; published 13 March 2008)

We investigate the chiral edge states in the two-dimensional ferromagnetic kagomé lattice with spin anisotropies included. The system is periodic in the x direction, but has two edges in the y direction. The Harper equation for solving the energies of edge states is derived. We find that there are two edge states in each bulk energy gap, corresponding to two zero points of the Bloch function on the complex-energy Riemann surface (RS). The edge-state energy loops parametrized by the momentum k_x flow across the holes of the RS. When the Fermi energy lies in the bulk energy gap, the quantized Hall conductance is given by the winding number of the edge states across the holes, which reads as $\sigma_{xy}^{\text{edge}}=-\frac{e^2}{h}\,\text{sgn}(\sin\phi)$, where ϕ is the spin-chiral parameter (see text). This result is consistent with that based on the topological bulk theory.

DOI: 10.1103/PhysRevB.77.125119 PACS number(s): 73.43.−f, 73.43.Cd, 71.27.+a

Recently, the quantum transport of electrons in spin-orbit coupled[1–3] or spin-chiral ferromagnetic systems[4–7] has been the focus of intense interest in condensed matter physics. One typical spin-chiral ferromagnetic system is represented by pyrochlore compounds $R_2Mo_2O_7$ (R=Nd, Sm, and Gd), in which the spin configuration is noncoplanar and the spin chirality appears. As a consequence, the quantum transport of electrons, especially the transverse conductivity σ_{xy}, is expected to be affected by the presence of spin chirality. Ohgushi *et al.*[8] have first pointed out that the chiral spin state can be realized by the introduction of spin anisotropy in an *ordered* spin system on the two-dimensional (2D) kagomé lattice, which is the cross section of the pyrochlore lattice perpendicular to the (1,1,1) direction.[9] In this case, it has been shown in the topological bulk theory[8,10] that the presence of a chiral spin state may induce a gauge-invariant nonzero Chern number, thus resulting in a quantized Hall effect in insulating state.

In this paper, we turn to study the 2D kagomé lattice with two edges, which, as will be shown below, displays two *chiral* (instead of *nonchiral*) edge states localized near the sample boundaries. Closely following the topological edge theory established in the past decade,[11–13] we first derive the transfer matrix (namely, the Harper equation[14–16]) for solving the energies of the edge states. Although the transfer matrix elements are no longer polynomials of the energy ϵ for a fixed spin-chiral parameter ϕ (except in special cases $\phi=0,\pm\pi/2,\pi$), we find that the transfer matrix method is also applicable in this system. Then by numerical calculation, we find that there are two edge states in each bulk energy gap, corresponding to two zero points of the Bloch function on the complex-energy Riemann surface (RS). Remarkably different from the case of a square lattice under a magnetic field,[11] the edge-state energy loops move *across* (*not around*) the holes in the RS in the present model. The two edge-state energy loops lying in the same energy gap are tangent at one point and their appearance shows an "∞" structure. Furthermore, we obtain that when the Fermi energy lies in the bulk energy gap, the quantum Hall conductance given by the winding number of the edge state can be written as $\sigma_{xy}^{\text{edge}}=-\frac{e^2}{h}\,\text{sgn}(\sin\phi)$. This result, based on the topological edge theory, is consistant with that based on the topological bulk theory.[8,10]

Following Ref. 8, we consider the double-exchange ferromagnet on the kagomé lattice schematically shown in the left panel of Fig. 1.[8,10] Here, the triangle is one face of the tetrahedron, and the easy axis of the spin anisotropy points to the center of each tetrahedron and has an out-of-plane component. In this situation, the three local spins on sites A, B, and C in the left panel of Fig. 1 have different directions and the spin chirality emerges. The effective Hamiltonian for the hopping electrons strongly Hund coupled to these localized spins is given by $H=\Sigma_{NN}t_{ij}^{eff}c_i^\dagger c_j$, with $t_{ij}^{eff}=t\langle\chi_i|\chi_j\rangle=te^{ia_{ij}}\cos\frac{\vartheta_{ij}}{2}$. Here, the spin wave function $|\chi_i\rangle$ is explicitly given by $|\chi_i\rangle=\left[\cos\frac{\vartheta_i}{2},e^{i\phi_i}\sin\frac{\vartheta_i}{2}\right]^T$, where the polar coordinates are pinned by the local spins, i.e., $\langle\chi_i|\mathbf{S}_i|\chi_i\rangle=\frac{1}{2}(\sin\vartheta_i\cos\phi_i,\sin\vartheta_i\sin\phi_i,\cos\vartheta_i)$. ϑ_{ij} is the angle between the two spins $\mathbf{S}_i$ and $\mathbf{S}_j$. The phase factor a_{ij} can be regarded as the gauge vector potential $a_\mu(\mathbf{r})$, and the corresponding gauge flux is related to scalar spin chirality $\chi_{ijk}=\mathbf{S}_i\cdot(\mathbf{S}_j\times\mathbf{S}_k)$.[17] In periodic crystal lattices, the nonvanishing of the gauge flux relies on the multiband structure with each band being characterized by a Chern number.[18,19] Following Refs. 8 and 10, we set the flux originated from the spin chirality per triangle (see Fig. 1) as ϕ, which satisfies $e^{i\phi}=e^{i(a_{AB}+a_{BC}+a_{CA})}$. The flux penetrating one hexagon is determined as -2ϕ. We take the gauge in which the phase of t_{ij}^{eff} is the same for all the nearest-neighbor pairs, with the direction shown by the arrows in the left panel of Fig. 1. It should be pointed out that the net flux through a unit cell vanishes due to the cancellation of the contribution of the two triangles and a hexagon. Also noted is that the time-reversal symmetry is broken except for cases of $\phi=0$ and π. In the following we change notation $i\rightarrow(lms)$, where (lm) label the kagomé unit cell and s denotes the sites A, B, and C in this cell. The size of the unit cell is set to be unity throughout this paper.

Now we suppose that the system is periodic in the x direction, but has two edges in the y direction (see the right

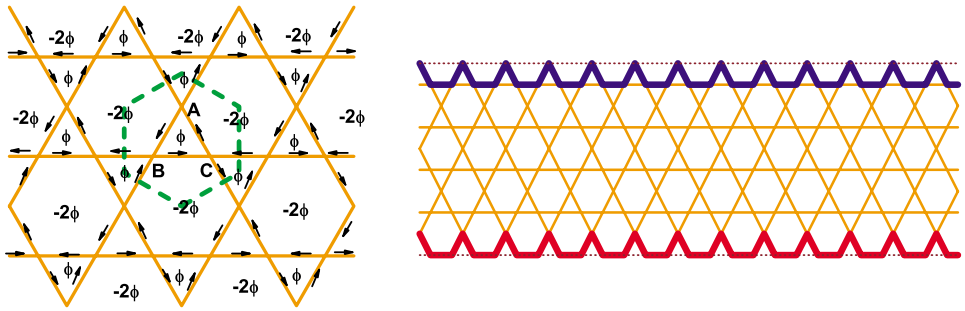

FIG. 1. (Color online) Left panel: Two-dimensional spin-chiral ferromagnetic kagomé lattice. The dashed line represents the Wigner-Seitz unit cell, which contains three independent sites (A, B, and C). It is assumed that each site has a different spin anisotropy axis. The arrows denote the sign of the phase of the transfer integral t_{ij}. Right panel: The 2D kagomé lattice system with edges along the y direction.

panel of Fig. 1). Since the system is periodic in the x direction, we can use a momentum representation of the electron operator

$$c_{(lms)} = \frac{1}{\sqrt{L_x}} \sum_{k_x} e^{ik_x X_{(lms)}} \gamma_{ms}(k_x), \tag{1}$$

where $(X_{(lms)}, Y_{(lms)})$ are the coordinate of the site s in the unit cell (lm), and k_x is the momentum along the x direction. Let us consider the one-particle state $|\Psi(k_x)\rangle = \Sigma_{ms} \Psi_{ms}(k_x) \gamma^{\dagger}_{ms}(k_x)|0\rangle$. Inserting it into the Schrödinger equation $H|\Psi\rangle = \epsilon|\Psi\rangle$, we can easily obtain the following three eigenvalue equations for sites A, B, and C:

$$\begin{aligned}
\epsilon \Psi_{mA} &= e^{-i\phi/3}[e^{i(1/4)k_x}\Psi_{mB} + e^{-i(1/4)k_x}\Psi_{(m+1)B}] \\
&\quad + e^{i\phi/3}[e^{-i(1/4)k_x}\Psi_{mC} + e^{i(1/4)k_x}\Psi_{(m+1)C}], \\
\epsilon \Psi_{mB} &= 2e^{-i\phi/3} \cos\left(\frac{k_x}{2}\right)\Psi_{mC} + e^{i\phi/3}[e^{-i(1/4)k_x}\Psi_{mA} \\
&\quad + e^{i(1/4)k_x}\Psi_{(m-1)A}], \\
\epsilon \Psi_{mC} &= e^{-i\phi/3}[e^{i(1/4)k_x}\Psi_{mA} + e^{-i(1/4)k_x}\Psi_{(m-1)A}] \\
&\quad + 2e^{i\phi/3} \cos\left(\frac{k_x}{2}\right)\Psi_{mB}.
\end{aligned} \tag{2}$$

Eliminating the B- and C-sublattice sites, we obtain the difference equation,

$$\begin{aligned}
&\left\{\epsilon^3 - 4\epsilon\left[1 + \cos^2\left(\frac{k_x}{2}\right)\right] - 8\cos^2\left(\frac{k_x}{2}\right)\cos\phi\right\}\Psi_{mA} \\
&\quad = 2\cos\left(\frac{k_x}{2}\right)(\epsilon + 2\cos\phi)[\Psi_{(m+1)A} + \Psi_{(m-1)A}].
\end{aligned} \tag{3}$$

This is the Harper equation.[14,15] Equation (3) can be represented in the following matrix form:

$$\begin{pmatrix} \Psi_{(m+1)A} \\ \Psi_{mA} \end{pmatrix} = \tilde{M}(\epsilon) \begin{pmatrix} \Psi_{mA} \\ \Psi_{(m-1)A} \end{pmatrix}, \tag{4}$$

where

$$\tilde{M}(\epsilon) = \begin{pmatrix} p & -1 \\ 1 & 0 \end{pmatrix} \tag{5}$$

and $p = \frac{\epsilon(\epsilon^2-4)}{2\cos(k_x/2)(\epsilon+2\cos\phi)} - 2\cos\left(\frac{k_x}{2}\right)$. In the following, we do not explicitly write the subscript A in Eq. (4). Then we get a reduced transfer matrix linking the two edges as follows:

$$\begin{pmatrix} \Psi_{L_y+1} \\ \Psi_{L_y} \end{pmatrix} = M(\epsilon) \begin{pmatrix} \Psi_1 \\ \Psi_0 \end{pmatrix}, \tag{6}$$

where

$$M(\epsilon) = \tilde{M}(\epsilon)^{L_y} = \begin{pmatrix} M_{11}(\epsilon) & M_{12}(\epsilon) \\ M_{21}(\epsilon) & M_{22}(\epsilon) \end{pmatrix}. \tag{7}$$

For general ϕ, which varies in the range between $-\pi$ and π, $M_{ij}(\epsilon)$ $(i, j=1$ and $2)$ are not polynomials of ϵ. At four special values, i.e., $\phi = 0, \pm\frac{\pi}{2}, \pi$, however, they can be written as polynomials of ϵ, with the degree of $2L_y$ for M_{11}, $2L_y - 1$ for M_{12} and M_{21}, and $2L_y - 2$ for M_{22}. In fact, in the spin-chiral cases of $\phi = \pm\frac{\pi}{2}$, the factor p in M_{ij} is reduced to $p = \frac{\epsilon^2-4}{2\cos(k_x/2)} - 2\cos\left(\frac{k_x}{2}\right)$. Whereas in the spin-nonchiral cases of $\phi = 0$ and π, the factor p in M_{ij} is reduced to $p = \frac{\epsilon(\epsilon\mp 2)}{2\cos(k_x/2)} - 2\cos\left(\frac{k_x}{2}\right)$. All kinds of solutions from Eq. (6) are obtained by different choices of Ψ_0 and Ψ_1.

Now we investigate the energy spectrum of the one-dimensional problem with special attention to the edge states. The boundary condition of this problem is

$$\Psi_{L_y} = \Psi_0 = 0. \tag{8}$$

With Eqs. (6) and (7), one can easily obtain that the solutions satisfy

$$M_{21}(\epsilon) = 0. \tag{9}$$

From

$$\begin{pmatrix} \Psi_{L_y+1} \\ \Psi_{L_y} \end{pmatrix} = \tilde{M}^2(\epsilon) \begin{pmatrix} \Psi_{L_y-1} \\ \Psi_{L_y-2} \end{pmatrix} = M(\epsilon) \begin{pmatrix} \Psi_1 \\ 0 \end{pmatrix},$$

one can find that

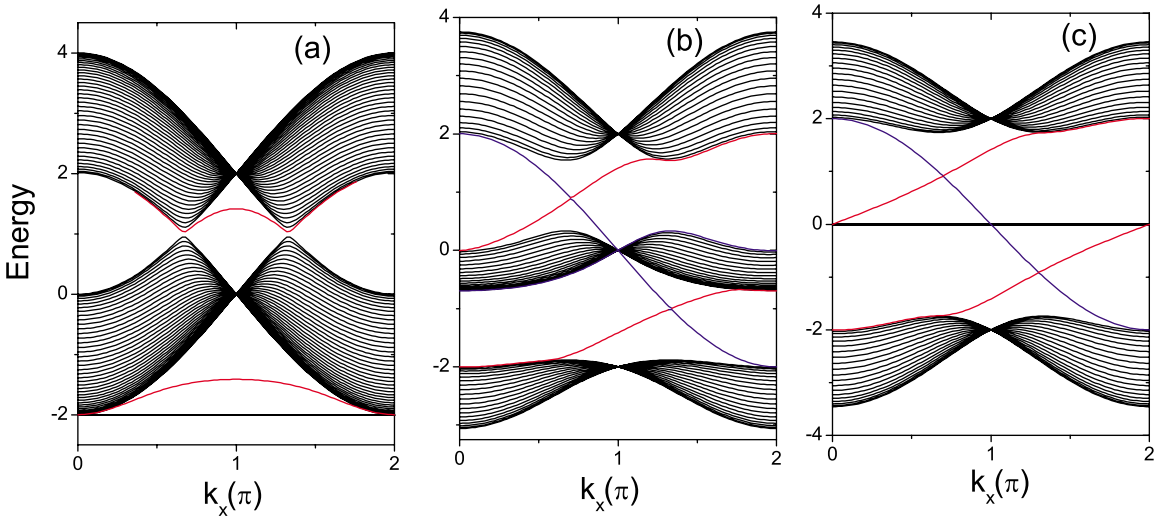

FIG. 2. (Color online) Energy spectrum of the two-dimensional spin-chiral ferromagnetic kagomé lattice system with fixed boundary under different spin-chiral parameters: (a) $\phi=0$, (b) $\phi=\pi/3$, and (c) $\phi=\pi/2$. The shaded areas are the energy bands and the colored lines are the spectrum of the edge states. The red and blue lines mean that the edge states are localized near $y\approx 1$ and $y\approx L_y-1$, respectively.

$$\Psi_{L_y-1} = -M_{11}(\epsilon)\Psi_1. \tag{10}$$

If we use a usual normalized wave function, the state is localized at the edges as

$$|M_{11}(\epsilon)| \ll 1 \quad \text{localized at } y \approx 1 \text{ (down edge)},$$

$$|M_{11}(\epsilon)| \gg 1 \quad \text{localized at } y \approx L_y - 1 \text{ (up edge)}. \tag{11}$$

Because the analytical derivation is very difficult, we now start a numerical calculation from Eq. (2) and draw in Fig. 2 the energy spectrum of the fixed boundary system as a function of k_x for three values of spin-chiral parameter ϕ. The number of sites A (or B or C) in the y direction is chosen to be $L_y=50$. Clearly, one can see that the edge states occur in the energy gaps or at the band edges. From Figs. 2(b) and 2(c), one can clearly observe that in the spin-chiral cases, i.e., $\phi\neq 0$ (or π), there are three dispersed energy bands (the shaded areas) with two edge states (the colored lines) lying in each energy gap. This feature is different from that in the case of the square lattice in an external magnetic field,[11] in which each gap has only one edge state. The reason for this difference is that the factor p in $M_{ij}(\epsilon)$ is no longer a linear function of ϵ in the present case.

Before studying the Hall conductance of this system, let us briefly review the winding number,[11,13] which is, as well as the Chern number, a well-defined topological quantity. Let us consider the bulk Bloch function at sites with y coordinate of L_y. For the Bloch function, $\Psi_1^{(b)}$ and $\Psi_0^{(b)}$ compose an eigenvector of M with the eigenvalue ρ,

$$M(\epsilon)\begin{pmatrix}\Psi_1^{(b)}\\ \Psi_0^{(b)}\end{pmatrix} = \rho(\epsilon)\begin{pmatrix}\Psi_1^{(b)}\\ \Psi_0^{(b)}\end{pmatrix}. \tag{12}$$

We extend the energy ϵ to a complex energy to discuss a wave function of the edge state. Here, we use complex variable z for the energy. From Eq. (12) we get

$$\rho(z) = \frac{1}{2}[\Delta(z) - \sqrt{\Delta^2(z)-4}] \tag{13}$$

and

$$\Psi_{L_y-1}(z) = -\frac{M_{11}(z)+M_{22}(z)-\sqrt{\Delta^2(z)-4}}{-M_{11}(z)+M_{22}(z)+\sqrt{\Delta^2(z)-4}}M_{21}(z), \tag{14}$$

where $\Delta(z)=\mathrm{Tr}[M(z)]$ and $\Psi_1=1$ are used. Since the analytic structure of the wave function is determined by $\omega=\sqrt{\Delta^2(z)-4}$, we consider the RS of a hyperelliptic curve $\omega^2=\Delta^2(z)-4$. To make the analytic structure of ω unique, we have to specify the branch cuts which are given by $\Delta^2(z)-4\leqslant 0$ at $\Im z=0$. Since this condition also gives the condition for $|\rho|=1$, the branch cuts are given by the three energy bands. Therefore, $\Delta^2(z)-4$ can be factorized as

$$\omega = \sqrt{\Delta^2(z)-4} = \sqrt{\prod_{i=1}^{6}(z-\lambda_i)},$$

where λ_i denote energies of the band edges. The RS is obtained by gluing the two Riemann spheres at these branch cuts along the arrows (see Fig. 3). The Riemann spheres are obtained by compactifying the $|z|=\infty$ points to one point. After the gluing operation, the surface is topologically equivalent to the surface shown in Fig. 4. In the present model, the genus of the RS is $g=2$, which is the number of energy gaps. In this way, the wave function is defined on the genus-2 RS $\Sigma_{g=2}(k_x)$. The branch of the function is specified as $\Delta^2(z)-4>0$ ($z\to-\infty$ on the real axis of R^+). Then if z lies in the jth gap from below on the real axis (notice that there are two real axes), $\alpha(-1)^j\sqrt{\Delta^2(z)-4}\geqslant 0$, z (real) on R^α ($\alpha=+,-$). So, at the energies of the edge states μ_j,

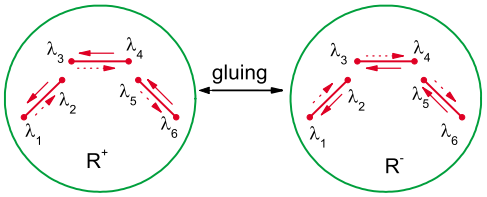

FIG. 3. (Color online) Two sheets (Riemann spheres) with 3 cuts which correspond to the energy bands of the system. The RS of the Bloch function is obtained by gluing the two spheres along the arrows near the cuts.

$$\sqrt{\Delta^2(\mu_j)-4} = \alpha(-1)^j|M_{11}(\mu_j)-M_{22}(\mu_j)| \quad (\mu_j \in R^\alpha,\ \alpha=+,-). \tag{15}$$

In addition, by simple calculation, we can also obtain

$$\Delta(\epsilon)\begin{cases} \leqslant -2 & \text{for } j \text{ odd} \\ \geqslant 2 & \text{for } j \text{ even,} \end{cases} \tag{16}$$

where the energy ϵ (on $R^{\pm}$) is in the jth gap. From Eqs. (15), (16), and (11), we can get that when the zero point is on the upper sheet of the RS, the edge state is localized at the down edge; when the zero point is on the lower sheet of the RS, the edge state is localized at the up edge.

In Fig. 4, on the RS, the energy gaps correspond to circles around the holes of the $\Sigma_{g=2}(k_x)$ and the energy bands correspond to closed paths on $\Sigma_{g=2}(k_x)$. The Bloch function is defined on this surface. $\Psi^{(b)}_{L_y-1}$ has always $2g=4$ zero points at the edge-state energy μ_j [$\Psi^{(b)}_{L_y-1}(\mu_j)=0$]. Since there are two real axes on the $\Sigma_{g=2}(k_x)$, there are eight μ_j's on the RS. However, only one of every two gives a zero of $\Psi^{(b)}_{L_y-1}$.

Changing k_x in one period, we can consider a family of $\Sigma_{g=2}(k_x)$. $\Sigma_{g=2}(k_x)$ can be modified by this change, yet all the $\Sigma_{g=2}(k_x)$ with different k_x's are topologically equivalent if there are stable energy gaps in the 2D spectrum. By identifying the topologically equivalent $\Sigma_{g=2}(k_x)$, we can observe that the $\mu_j(k_x)$ moves across the holes and forms an oriented loop $C(\mu_j)$. Note that the present case is prominently different from the previous case of the square lattice under an external magnetic field,[11] in which μ_j moves *around* the holes due to the fact that the edge state μ_j links two bands in

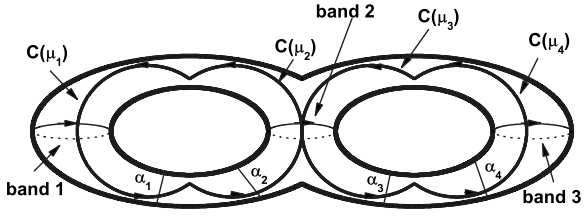

FIG. 4. The RS of the Bloch function. $C(\mu_j)$ is a loop formed by the trace of the zero point of $\Psi_{L_y-1}(z)$. The energy bands are shown by closed loops. The corresponding winding numbers are $I(C(\mu_j))=1$ for all j.

one period of k_x. The two edge-state energy loops C's in the same energy gap are tangent at one point and their appearance shows a ∞ structure, as shown in Fig. 4.

As pointed out by Hatsugai,[11,13] when the Fermi energy ϵ_F of the 2D system lies in the ith energy gap, the Hall conductance is given by the winding number of the edge state, which is given by the number of intersections $I(\alpha_i, C(\mu_i))$ [$\equiv I(C(\mu_i))$] between the canonical loop α_i on the RS and the trace of μ_i. In the present model, because there are two edge states and, correspondingly, there are two canonical loops in one energy gap, the Hall conductance by its definition can be written as

$$\sigma_{xy}^{j,\text{edge}} = \begin{cases} -\dfrac{e^2}{h} I(C(\mu_{2j-1})), & \epsilon_F \leqslant \epsilon_{T_j} \\ -\dfrac{e^2}{h} I(C(\mu_{2j})), & \epsilon_F > \epsilon_{T_j}, \end{cases} \tag{17}$$

where ϵ_{T_j} is the energy at the tangent point in the jth energy gap. Similarly, this expression can be obtained by the Byers-Yang formula:[20] Suppose that one increases an external magnetic flux Φ from 0 to 1 adiabatically. According to the Laughlin-Halperin argument,[21,22] when the Fermi energy lies in the jth energy gap and $\epsilon_F \leqslant \epsilon_{T_j}$ [or $\epsilon_F > \epsilon_{T_j}$], $I(C(\mu_{2j-1}))$ [or $I(C(\mu_{2j}))$] states are carried from the down edge ($y=1$) to the up edge ($y=L_y-1$) in net. The energy change during the adiabatic process is $\Delta E = I(C(\mu_{2j-1}))(-e)V_y$ [or $\Delta E = I(C(\mu_{2j}))(-e)V_y$], where V_y is a voltage in the y direction. This gives the Hall current I_x as follows:

$$I_x = c\frac{\Delta E}{\Phi_0 \Delta \Phi} = \sigma_{xy} V_y, \tag{18}$$

where $\Phi_0 = hc/e$ is the flux quantum. Then we get an expression for $\sigma_{xy}^{\text{edge}}$ as Eq. (17).

On the genus $g=2$ RS, the first homotopy group is generated by $4g=8$ generators, α_i and β_i, $i=1,\ldots,4$. We can observe that μ_{2j-1} (μ_{2j}) moves *one* time across the jth hole, which means $C(\mu_{2j-1})$ [$C(\mu_{2j})$] $\approx \beta_j$ and $|I(C(\mu_{2j-1}))|$ [$|I(C(\mu_{2j}))|$] $=1$. Considering winding direction (see Fig. 5 in Ref. 11), one can obtain that $I(C(\mu_i))=1$ when $\phi \in (0,\pi)$, while $I(C(\mu_i))=-1$ when $\phi \in (-\pi, 0)$ for all i. So, $I(C(\mu_i)) = \text{sgn}(\sin\phi)$ and

$$\sigma_{xy}^{1,\text{edge}} = \sigma_{xy}^{2,\text{edge}} = -\frac{e^2}{h}\,\text{sgn}(\sin\phi). \tag{19}$$

Now we turn back to make an analysis of Fig. 2 with the help of the above results. At $\phi=0$, the lower energy band becomes dispersionless [Fig. 2(a)], which reflects the fact that the 2D kagomé lattice is a line graph of the honeycomb structure.[23] This flat band touches at $k_x=0$ with the middle band, while the middle band touches at $k_x=\frac{2\pi}{3}$ and $\frac{4\pi}{3}$ with the upper band. So there are no bulk energy gaps, and the Hall conductance is zero in this case. At $\phi \neq 0$ and π, the 2D kagomé lattice has spin chirality, and there occur two bulk band gaps, as shown in Fig. 2(b) for $\phi=\pi/3$ and Fig. 2(c) for $\phi=\pi/2$. Then according to Eq. (19), one can obtain that when the Fermi energy lies in the bulk gaps, $\sigma_{xy}^{1,\text{edge}} = \sigma_{xy}^{2,\text{edge}}$

$=-\frac{e^2}{h}$. Note that in the case of $\phi=\frac{\pi}{2}$, the middle energy band becomes flat [Fig. 2(c)] due to the particle-hole symmetry.

Finally, let us compare $\sigma_{xy}^{\text{edge}}$ [Eq. (19)] in the present model with that in the bulk theory.[8,10] In the latter, the bulk Hall conductance has been derived to be $\sigma_{xy}^{1,\text{band}}=-\frac{e^2}{h}\,\text{sgn}(\sin\phi)$, $\sigma_{xy}^{2,\text{band}}=0$, and $\sigma_{xy}^{3,\text{band}}=\frac{e^2}{h}\,\text{sgn}(\sin\phi)$ for the three bands. So, when the Fermi energy ϵ_F lies in the ith energy gap, the bulk Hall conductance $\sigma_{xy}^{i,\text{bulk}}$ is given by

$$\sigma_{xy}^{i,\text{bulk}}=\sum_{j=1}^{i}\sigma_{xy}^{j,\text{band}}=-\frac{e^2}{h}\,\text{sgn}(\sin\phi), \tag{20}$$

where $i=1$ and 2. Comparing Eq. (20) with Eq. (19), one can obtain

$$\sigma_{xy}^{\text{edge}}=\sigma_{xy}^{\text{bulk}}, \tag{21}$$

which is in accord with the recently established common recognition on the Hall conductance in the systems with and without edges.

Note that the gapless edge states in the truncated kagomé lattice are topologically stable against random-potential perturbation, provided that the perturbation is small compared to the bulk gaps. We have numerically confirmed this point. Actually, the key factor for the emergence of the two edge states in each gap and their consequent crossing in the gap is the spin-chiral parameter ϕ, which is determined by the coupling between conduction electrons and local magnetic moment on each site of the lattice. In the present treatment, the local Hund's exchange interaction J_0 (between the conduction electrons and the local spins) has been assumed infinite, which completely polarizes the spins of conduction electrons and results in the description of conduction electrons in terms of the spinless fermions and the effective three-band model. In other words, we are treating the case of infinite Mott gap. From this sense, a more realistic treatment is to take into account the finite exchange interaction and, thus, to explicitly include the spin degrees of freedom in a six-band model. In this case, the winding features of the edge states below the Mott gap are expected to differ from those in the present paper and, thus, it will be interesting to study the different behaviors of the edge states by tuning the exchange field from the weak to the strong cases (compared to the electron hopping energy t). However, the crossing property of the two edge states remains unchanged upon the inclusion of finite J_0. The subsequent finite Mott gap also remains trivial, in the sense the topological edge states in the Mott gap will not appear. Besides the ratio J_0/t being an interesting energy scale, the amplitude of temperature provides the other energy scale to determine the validity of the present model we used. In particular, at high temperature, due to the spin wave excitation, the present approximation of frozen electron spins aligning with the local magnetic moments turns to be invalid, and the effect of spin fluctuation should be properly accounted for. We would like to leave these open issues for future studies.

In summary, we have investigated the effect of the chiral edge states on the quantum Hall conductance in the 2D kagomé lattice with edges. According to our derived Harper equation, there are two edge states lying in each energy gap. They are tangent at one point in the gap, thus showing an ∞ structure. The energy loops for these two edge states move across the holes in the RS. We have also analyzed the winding number of these two edge states, which gives the quantum Hall conductance $\sigma_{xy}^{\text{edge}}=-\frac{e^2}{h}\,\text{sgn}(\sin\phi)$ when the Fermi energy lies in the bulk gap. This conclusion is consistent with that based on the topological bulk Chern-number theory.

This work was supported by NSFC under Grants Nos. 10604010 and 60776063.

*Corresponding author. zhang_ping@iapcm.ac.cn

[1] T. Jungwirth, Q. Niu, and A. H. MacDonald, Phys. Rev. Lett. **88**, 207208 (2002).
[2] Z. Fang, N. Nagaosa, K. S. Takahashi, A. Asamitsu, R. Mathieu, T. Ogasawara, H. Yamada, M. Kawasaki, Y. Tokura, and K. Terakura, Science **302**, 92 (2003).
[3] Y. Yao, L. Kleinman, A. H. MacDonald, J. Sinova, T. Jungwirth, D.-S. Wang, E. Wang, and Q. Niu, Phys. Rev. Lett. **92**, 037204 (2004).
[4] P. Matl, N. P. Ong, Y. F. Yan, Y. Q. Li, D. Studebaker, T. Baum, and G. Doubinina, Phys. Rev. B **57**, 10248 (1998).
[5] S. H. Chun, M. B. Salamon, Y. Lyanda-Geller, P. M. Goldbart, and P. D. Han, Phys. Rev. Lett. **84**, 757 (2000).
[6] J. Ye, Y. B. Kim, A. J. Millis, B. I. Shraiman, P. Majumdar, and Z. Tešanović, Phys. Rev. Lett. **83**, 3737 (1999).
[7] Y. Taguchi, Y. Oohara, H. Yoshizawa, N. Nagaosa, and Y. Tokura, Science **291**, 2573 (2001).
[8] K. Ohgushi, S. Murakami, and N. Nagaosa, Phys. Rev. B **62**, R6065 (2000).
[9] A. P. Ramirez, Annu. Rev. Mater. Sci. **24**, 453 (1994).
[10] Z. Wang and P. Zhang, Phys. Rev. B **76**, 064406 (2007).
[11] Y. Hatsugai, Phys. Rev. B **48**, 11851 (1993).
[12] Y. Hatsugai, Bull. Am. Phys. Soc. **38**, 397 (1993).
[13] Y. Hatsugai, Phys. Rev. Lett. **71**, 3697 (1993).
[14] P. G. Harper, Proc. Phys. Soc., London, Sect. A **68**, 874 (1955).
[15] D. R. Hosfstadter, Phys. Rev. B **14**, 2239 (1976).
[16] G. H. Wannier, Phys. Status Solidi B **88**, 757 (1978); G. H. Wannier, G. M. Obemaier, and R. Ray, *ibid.* **93**, 337 (1979).
[17] V. Kalmeyer and R. B. Laughlin, Phys. Rev. Lett. **59**, 2095 (1987); G. Baskaran and P. W. Anderson, Phys. Rev. B **37**, 580 (1988); R. B. Laughlin, Science **242**, 525 (1988); X. G. Wen, F. Wilczek, and A. Zee, Phys. Rev. B **39**, 11413 (1989).
[18] D. J. Thouless, *Topological Quantum Numbers in Nonrelativistic Physics* (World Scientific, Singapore, 1998).
[19] R. Shindou and N. Nagaosa, Phys. Rev. Lett. **87**, 116801 (2001).
[20] N. Byers and C. N. Yang, Phys. Rev. Lett. **7**, 46 (1961).
[21] R. B. Laughlin, Phys. Rev. B **23**, 5632 (1981).
[22] B. I. Halperin, Phys. Rev. B **25**, 2185 (1982).
[23] A. Mielke, J. Phys. A **24**, L73 (1991); **24**, 3311 (1991); **25**, 4335 (1992).